Applied Catalysis B: Environmental 90 (2009) 38–44

Contents lists available at ScienceDirect

Applied Catalysis B: Environmental

journal homepage: www.elsevier.com/locate/apcatb

Design of a stable steam reforming catalyst—A promising route to sustainable hydrogen from biomass oxygenates

B. Matas Güell [a], I. Babich [a], K.P. Nichols [b], J.G.E. Gardeniers [b], L. Lefferts [a], K. Seshan [a,*]

[a] Catalytic Processes & Materials, Faculty of Science and Technology, University of Twente, PO Box 217, 7500 AE, Enschede, The Netherlands
[b] Mesoscale Chemical Systems, Faculty of Science and Technology, University of Twente, PO Box 217, 7500 AE, Enschede, The Netherlands

ARTICLE INFO

Article history:
Received 19 December 2008
Received in revised form 9 February 2009
Accepted 13 February 2009
Available online 21 February 2009

Keywords:
Sustainable
Hydrogen
Steam reforming
Pt
Oxygen
MALDI-TOF MS

ABSTRACT

The influence of the support and the presence of oxygen were investigated in the steam reforming of acetic acid, a bio-oil model compound, over Pt/ZrO_2 and Pt/CeO_2 catalysts. In the absence of oxygen, all catalysts suffered from deactivation. Acetone, formed *via* condensation/dehydration of acetic acid, is a coke precursor and causes catalyst deactivation. The use of a support with red-ox properties and the presence of oxygen improved the stability of the Pt/CeO_2 catalyst tremendously. Matrix-assisted laser desorption/ionization time-of-flight mass spectrometry (MALDI-TOF MS) characterization of coke indicates that the presence of oxygen prevents extensive oligomerization/coke forming reactions and that the resulting specie are more easily combusted.

© 2009 Elsevier B.V. All rights reserved.

1. Introduction

The concept of hydrogen as energy carrier is currently of interest, particularly within the context of sustainable development [1,2]. Biomass has recently drawn attention as a renewable hydrogen source, i.e., with no net contribution to CO_2 emissions. In the context of biomass, flash pyrolysis of lignocelluloses results in liquid bio-oil, a convenient feedstock for storage, transport and processing [3]. Catalytic steam reforming followed by water-gas shift is a standard commercial route and can be applied to maximize hydrogen yield from bio-oil. The complexity of bio-oils makes it difficult to design catalysts based on kinetic and spectroscopic studies and to establish reaction mechanisms. Thus, model representative compounds are often used. In this context, in the steam reforming of acetic acid, a major compound in bio-oil [3–5], we have previously shown excellent activity for Pt/ZrO_2 at relatively low temperatures (450 °C) [6]. However, catalyst stability was a major problem and Pt/ZrO_2 suffered from rapid deactivation. Based on our previous studies [6–8], we can generally conclude that higher temperatures, close to natural gas reforming, are required to minimize coking and extend catalyst stability.

We proposed earlier a bi-functional mechanism [6,7] where Pt and ZrO_2 are involved in the steam reforming of acetic acid (AcOH). The role of ZrO_2 is in the activation of water forming hydroxyl groups. However, acetic acid undergoes condensation/dehydration reactions on ZrO_2 resulting in the formation of carbonaceous deposits that cause deactivation. In this respect, a thorough understanding of the coke formation is fundamental to understand the deactivation mechanism and to design stable catalysts.

It is reported [9,10] that catalyst stability for steam reforming can be improved by the addition of small amounts of oxygen. Cavallaro et al. [9] reported a better stability for Rh/Al_2O_3 during the steam reforming of ethanol when ca. 3% O_2 was added to the reaction mixture. The positive effect was attributed to the *in situ* combustion of carbonaceous specie formed during reaction. Further, de Lima et al. [10] have recently reported improvement in the $Pt/CeZrO_2$ stability for the steam reforming of ethanol, when adding oxygen in the feed (O_2/ethanol molar ratio of 0.5). Oxygen availability for gasification of coke deposited on the support can be enhanced by using reducible supports such as CeO_2 [11,12]. Ability of these metal oxides to store and release oxygen, the so-called "oxygen storage capacity (OSC)" [12–14], may help to minimize/prevent coke accumulation and result in more stable catalysts.

Current research aims at improving the catalytic stability of Pt-based catalysts for steam reforming of acetic acid. Two approaches were identified: i.e., (i) use of oxide supports with red-ox properties, for e.g., CeO_2 and (ii) carrying out reforming under mild autothermal conditions i.e., introducing low amounts of O_2 in the feed. Matrix-assisted laser desorption/ionization time-of-flight mass spectrometry (MALDI-TOF MS) characterization of the coke

* Corresponding author.
E-mail address: k.seshan@utwente.nl (K. Seshan).

0926-3373/$ – see front matter © 2009 Elsevier B.V. All rights reserved.
doi:10.1016/j.apcatb.2009.02.008

allows an insight in the mechanism of coke formation, or in the relationship between coke properties and deactivation.

2. Experimental

2.1. Catalyst preparation

Catalysts were prepared by wet impregnation technique. An aqueous solution of $H_2PtCl_6{\cdot}6H_2O$ was used (Alfa Aesar). ZrO_2 (Daiichi Kigenso Kagaku Kogio, RC 100) and CeO_2 (Aldrich) were first calcined for 15 h at 850 °C (heating rate 5 °C min^{-1}) in flowing air (30 ml min^{-1}). The supports were then crushed and sieved to give grains of 0.3–0.6 mm. The grains were impregnated with the $H_2PtCl_6{\cdot}6H_2O$ solution to yield to 0.5 wt% Pt. The catalysts were dried for 4 h at 70 °C in vacuum and subsequently calcined at 725 °C for 15 h (heating rate 5 °C min^{-1}) in flowing air (30 ml min^{-1}).

2.2. Catalyst characterization

The elemental compositions of the catalysts were determined with X-ray fluorescence spectroscopy (XRF) (Phillips PW 1480 spectrometer). Specific surface area measurements were carried out by the BET method (Micromeritics TriStar).

H_2 chemisorption (Chemisorb 2750, Micromeritics) measurements were carried out to determine the Pt dispersions. Reducibility of the catalysts and supports was probed using temperature-programmed reduction (TPR) equipped with thermal conductivity detector (TCD). For this purpose, 50 mg of catalyst sample was pretreated in Ar at 700 °C for 5 min. After pretreatment, the sample was first cooled down to room temperature in Ar and then heated to 800 °C at a rate of 5 °C min^{-1} in a 5% H_2/Ar flow (30 ml min^{-1}).

The red-ox changes of CeO_2 during sequential reduction/oxidation treatments in hydrogen and water, respectively, were also tested in the same TPR setup. About 100 mg of Pt/CeO_2 was first heated to 900 °C in 5% H_2/Ar at 5 °C min^{-1} and then purged with He for 15 min at the same temperature. Subsequently, the gas flow was changed to 2.3% H_2O/He and the catalyst was cooled down to 50 °C. After purging the system with He for 15 min, the sample was heated again to 900 °C in 5% H_2/Ar at 5 °C min^{-1}.

Temperature program oxidation (TPO) experiments were performed to quantify the amount of coke deposits on the used catalyst. Samples were heated from room temperature to 800 °C in 1% O_2/Ar at 5 °C min^{-1}. Carbonaceous deposits were oxidized to CO_x, which passed through a methanator and was finally detected with a flame ionization detector (FID). This enables to differentiate between oxygen consumption during TPO for coke removal or re-oxidation of ceria.

For MALDI-TOF MS analysis, the method of Sievers et al. [15] was utilized, with only slight modifications. 10 mg of the spent catalyst was suspended in 250 μl of 1% trifluoroacetic acid solution (HPLC Grade, from Fisher Scientific) and 250 μl of 10 mg/ml 2,5-dihydrobenzoic acid (DHB) (Sigma–Aldrich). The solution was mixed for 30 s using a vortex mixer, ultrasonicated for 30 min, and centrifuged for 30 s at 1000 RPM. 2 μl of supernatant was pipetted onto a stainless steel MALDI plate, and mass spectra were recorded using a Waters SYNAPT HDMS MALDI-TOF mass spectrometer (Waters, USA). The spectrometer was operated in positive ion mode, and was calibrated using a polyethylene glycol (PEG) standard.

2.3. Catalytic testing

For catalytic experiments, 100 mg of catalyst with grains of 0.3–0.6 mm was loaded in a fixed-bed reactor (4 mm i.d.) and held by quartz wool plugs. The catalyst was first reduced *in situ* in 5% H_2/N_2 flow (50 ml min^{-1}) at 550 °C for 1 h. After purging with N_2 for 15 min, the temperature was increased to 700 °C. An aqueous solution of acetic acid with a steam to carbon molar ratio (S/C) of 5 was delivered by a pulse-free syringe pump (Isco Model 500 D). This solution was evaporated at 190 °C in a gasifier before entering the reactor. Nitrogen was used both as an inert carrier gas and as an internal standard. The feed delivery system was heated at 175 °C to avoid condensation. The gas feed, consisting of 2.5% CH_3COOH/25% H_2O/balance N_2, was introduced to the fixed-bed reactor. For continuous flow experiments in which oxygen was added in the stream, the gas mixture composition was 2.5% CH_3COOH/25% H_2O/1% O_2/balance N_2. For blank experiments, 100 mg of quartz particles was loaded in the fixed-bed reactor and held by quartz wool plugs. The total gas hourly space velocity (GHSV) was calculated on a volume basis (80 000 h^{-1}).

The composition of the product mixture was determined with an online gas chromatograph (GC, Varian CP-3800) equipped with Hayesep Q, Hayesep T, Molsieve 13X, Molsieve 5A and CP-Wax 52CB columns for separation. For the quantification of permanent gases, two TCDs were used, while for quantification of the hydrocarbons an FID was applied.

Acetic acid conversion was calculated as the number of moles of acetic acid reacted divided by the number of moles of acetic acid fed.

$$CH_3COOH + 2H_2O \rightarrow 2CO_2 + 4H_2 \quad (1)$$

The hydrogen yield was defined as the percentage of the maximum amount of hydrogen that can be produced, based on Eq. (1). For carbon-containing compounds, the yields were calculated based on C_1 equivalent values.

3. Results

3.1. Catalyst characterization

Physico-chemical characteristics of the catalysts are summarized in Table 1. The two catalysts had comparable Pt loadings (~0.5 wt%), dispersions (14–16%) and BET surface area of around 18 m^2/g. This allows realistic comparison of the two catalysts in their catalytic performance.

The hydrogen uptake by Pt/ZrO_2 and Pt/CeO_2 as a function of temperature is shown in Fig. 1. The peak around 250 °C in both

Table 1
Metal loading, Pt dispersion and BET surface area of the catalysts used in this work.

Catalyst	Pt content (%)	Dispersion (%)	Surface area (m^2/g)
Pt/ZrO_2	0.52	16	17.1
Pt/CeO_2	0.55	14	18.2

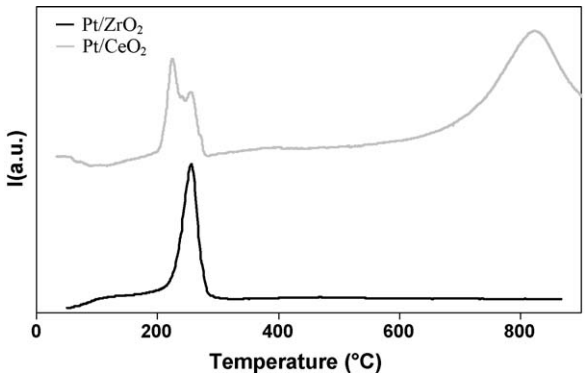

Fig. 1. Temperature program reduction of fresh preheated Pt/ZrO_2 and Pt/CeO_2.

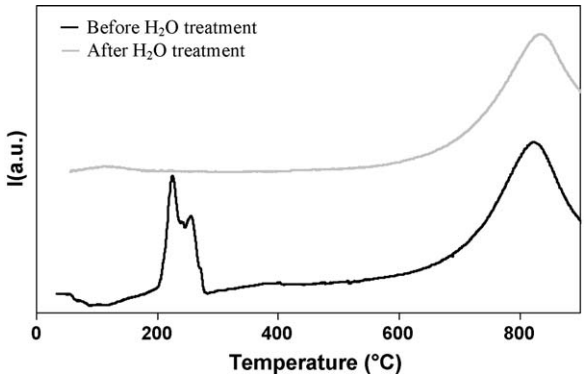

Fig. 2. Temperature program reduction of fresh preheated Pt/CeO_2 and Pt/CeO_2 re-oxidized by water after being previously reduced.

cases corresponds to reduction of platina. In the case of Pt/ZrO_2 no reduction peak for ZrO_2 was observed. In the Pt/CeO_2, the CeO_2 showed broad and significant reduction starting from around 500 °C. This peak is due to the reduction of lattice oxygen of CeO_2 [16–18]. The TPR profiles clearly show that only CeO_2 allows redox changes at the reaction temperature used in this study (700 °C).

TPR profiles of (i) a freshly calcined Pt/CeO_2 catalyst and (ii) the resulting reduced catalyst after exposure to water are shown in Fig. 2. It can be seen from the figure that the reduction peak, around 830 °C, reappears indicating re-oxidation of ceria with water during exposure at 700 °C and cooling down. Re-oxidation of Pt was not observed during this experiment.

3.2. Catalytic measurements

Product distribution of homogeneous decomposition of AcOH during time on stream (TOS) is shown in Fig. 3a. Approximately, 20% conversion of AcOH occurred and the only gas products observed were H_2, CO, and CO_2. This indicates that AcOH undergoes thermal decomposition at 700 °C. Higher AcOH conversions (~50%) were observed when 1% O_2 was added in the gas stream (Fig. 3b). This increase in conversion resulted in higher CO and CO_2 yields. Only traces of hydrogen were detected. Oxygen consumption was complete in all experiments. Carbon balance was ~85% in both cases, indicating that part of the acetic acid was converted to some by-products undetected during analysis.

3.2.1. Steam reforming of acetic acid over ZrO_2 and Pt/ZrO_2

Fig. 4a shows AcOH conversion and product yields during steam reforming over ZrO_2 at 700 °C. At initial TOS, AcOH was almost completely converted (95%) to CO_2, CH_4, H_2 and CO. After 30 min TOS, significant amounts of acetone were detected in the product stream, but disappeared after approximately 45 min TOS. Rapid deactivation of the catalyst was apparent during this period as evidenced by the decrease in AcOH conversion and gas yields. After 1 h TOS the system reached steady state, with AcOH conversion and product distribution similar to that due to gas phase reactions (Fig. 3a). The addition of 1% O_2 (Fig. 4b) resulted only in a slight increase of CO and decrease in H_2 and CH_4 yields. Acetone was observed again but deactivation occurred to a lesser extent. After 1 h TOS the conversion and product distribution remained unchanged and were similar to the results obtained during thermal cracking of acetic acid with the presence of oxygen.

Fig. 5a represents a typical experimental result of steam reforming of AcOH over Pt/ZrO_2 at 700 °C. As can be seen, product distribution is completely different from that with ZrO_2 (Fig. 4a) and changed drastically in time. Initially, AcOH was mostly converted to H_2 and CO_2; CO and CH_4 were observed in smaller amounts. After 40 min TOS acetone was observed as a product. At that time, H_2 and CO_2 yields decreased significantly. CO decreased to a lesser extent. CH_4 practically disappeared. After 3.5 h TOS the

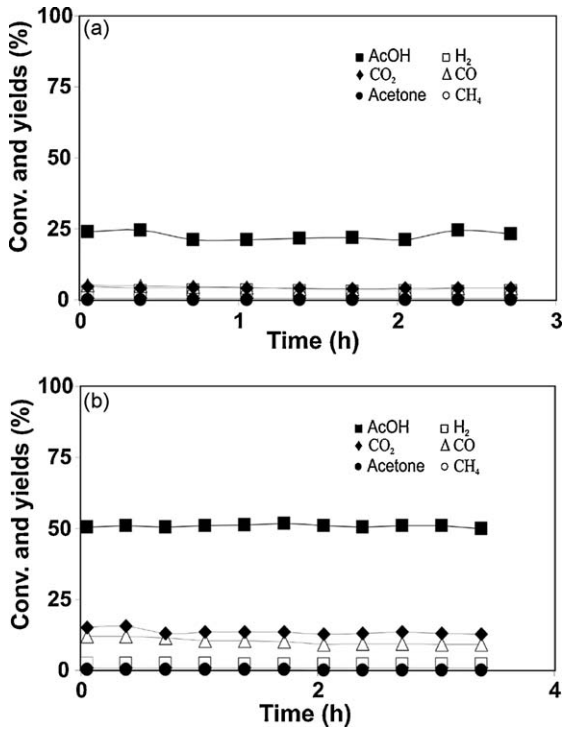

Fig. 3. Conversion and yields vs. time on stream for the steam reforming of AcOH over quartz particles in the absence (a) and presence (b) of oxygen (1% O_2). Reaction conditions: 700 °C, S/C = 5, and GHSV = 80 000 h^{-1}.

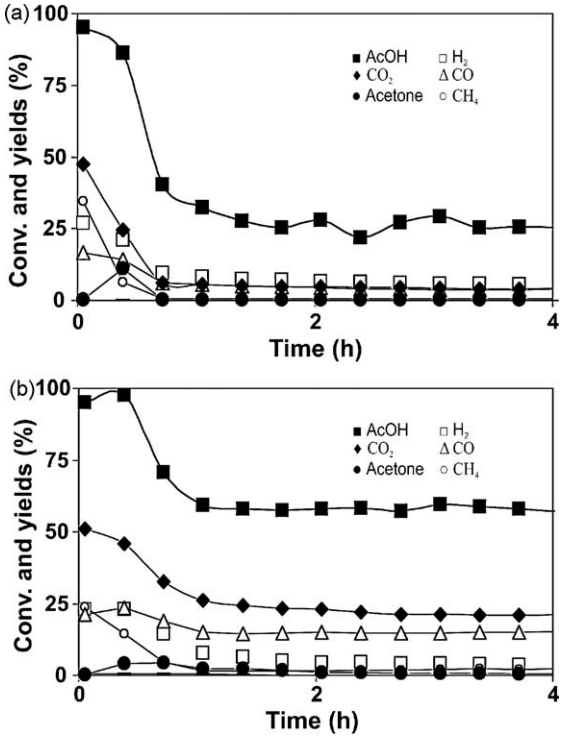

Fig. 4. Conversion and yields vs. time on stream for the steam reforming of AcOH over ZrO_2 in the absence (a) and presence (b) of oxygen (1% O_2). Reaction conditions: 700 °C, S/C = 5, and GHSV = 80 000 h^{-1}.

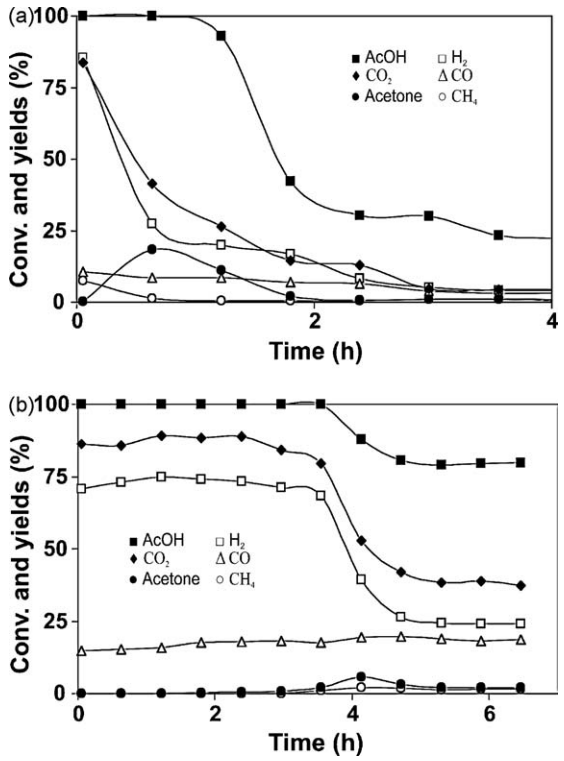

Fig. 5. Conversion and yields vs. time on stream for the steam reforming of AcOH over Pt/ZrO_2 in the absence (a) and presence (b) of oxygen (1% O_2). Reaction conditions: 700 °C, S/C = 5, and GHSV = 80 000 h^{-1}).

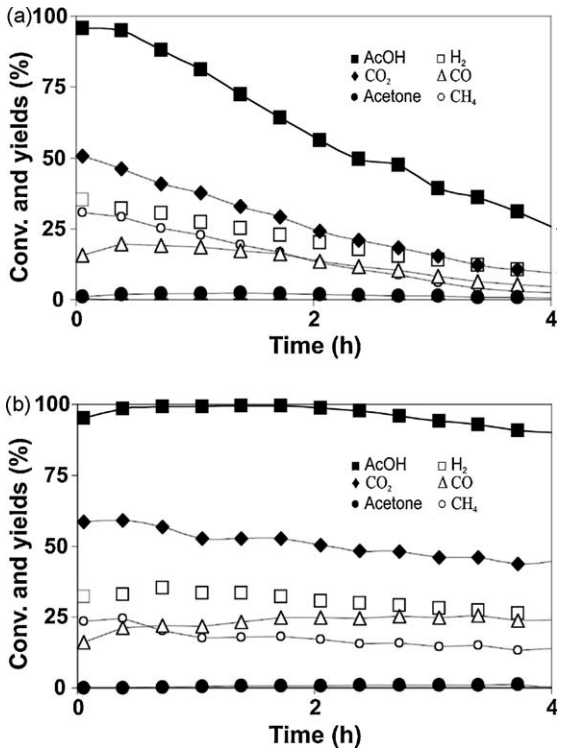

Fig. 6. Conversion and yields vs. time on stream for the steam reforming of AcOH over CeO_2 in the absence (a) and presence (b) of oxygen (1% O_2). Reaction conditions: 700 °C, S/C = 5, and GHSV = 80 000 h^{-1}.

system reached steady state. AcOH conversion decreased to 23%, which corresponded to gas phase thermal decomposition of AcOH.

The influence of oxygen on Pt/ZrO_2 is shown in Fig. 5b. The complete conversion of AcOH during the first 3.5 h TOS clearly shows an improvement in catalyst lifetime as compared to steam reforming without oxygen. During this period of time (3.5 h), only steam reforming products (H_2, CO_2 and CO) were observed. The addition of O_2 to the reaction mixture resulted in slightly higher CO and CO_2 yields. H_2 yield decreased from 85% to 70%. Again, the observation of a rapid decrease in conversion and gas product yields after 3.5 h TOS was evidence for catalyst deactivation. Acetone appeared in the gas phase during deactivation, reaching a maximum at 4 h TOS. These changes led to a new steady state that clearly differed from the product distribution corresponding to thermal cracking of AcOH in the presence of oxygen.

3.2.2. Steam reforming of acetic acid over CeO_2 and Pt/CeO_2

Fig. 6a shows AcOH conversion and product yields over CeO_2 at 700 °C. Initial AcOH conversion was nearly complete, leading to CO_2, H_2, CH_4 and CO. In contrast to ZrO_2, deactivation of CeO_2 occurred more gradually. Another significant difference between the two supports is that smaller amounts of acetone were observed over CeO_2. The effect of adding 1% O_2 in the steam reforming of AcOH over CeO_2 is illustrated in Fig. 6b. Complete conversion of AcOH was achieved during the first 2 h of reaction. CO_2, H_2, CH_4 and CO were observed as products. The stability of CeO_2 was improved, as evidenced by the reasonably stable product yields during the 4 h TOS.

Catalytic performance of Pt/CeO_2 is shown in Fig. 7a. This catalyst also showed very high initial activity with product yields close to thermodynamic equilibrium [i.e., H_2 (92% yield) and CO_2 (79% yield)]. Traces of acetone were observed. However, Pt/CeO_2 was more stable catalyst for the steam reforming than Pt/ZrO_2 under identical conditions and deactivated more gradually during the 10 h TOS measured (Figs. 5a and 7a).

In the presence of O_2 (Fig. 7b), interestingly, Pt/CeO_2 showed excellent stability in terms of H_2 production. No deactivation was observed during the 10 h TOS. Steam reforming and WGS products [H_2 (75% yield), CO (16% yield) and CO_2 (75%

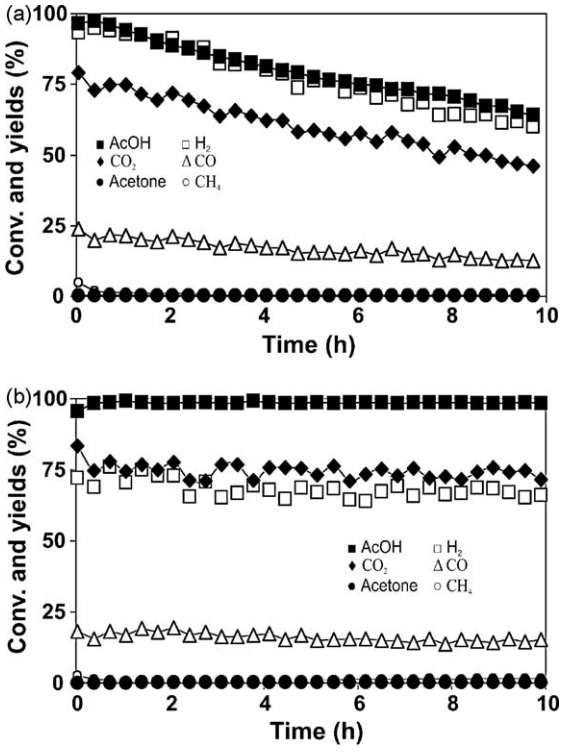

Fig. 7. Conversion and yields vs. time on stream for the steam reforming of AcOH over Pt/CeO_2 in the absence (a) and presence (b) of oxygen (1% O_2). Reaction conditions: 700 °C, S/C = 5, and GHSV = 80 000 h^{-1}.

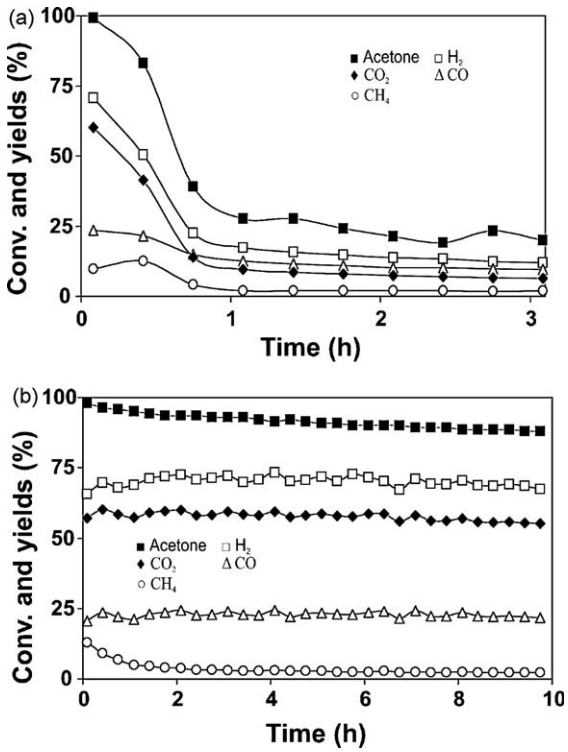

Fig. 8. Conversion and yields vs. time on stream for the steam reforming of acetone over Pt/ZrO_2 (a) and Pt/CeO_2 (b). Reaction conditions: 700 °C, S/C = 5, and GHSV = 96 000 h^{-1}.

yield)] were the only gases observed throughout the experiment.

3.2.3. Steam reforming of acetone over Pt/ZrO_2 and Pt/CeO_2

Fig. 8a shows the conversion and product distribution during steam reforming of acetone over Pt/ZrO_2 at 700 °C. Very high activity was observed in the beginning of the reaction, with complete conversion of acetone. Similar to the steam reforming of AcOH, H_2 and CO_2 were observed as main products, with yields around 70% and 60%, respectively. CO (25% yield) and CH_4 (10% yield) were detected in lower amounts. Drastic catalyst deactivation was noticed after few minutes of reaction. This resulted in a new steady state in which only 20% acetone was converted. The products were H_2, CO_2 and CO.

Like Pt/ZrO_2, steam reforming of acetone over Pt/CeO_2 (Fig. 8b) resulted in complete acetone conversion at initial TOS and comparable product distribution. However, using CeO_2 as a support improved the catalyst stability greatly. No decrease in H_2 yield was observed during 10 h TOS.

3.3. Characterization of deactivated catalysts

The amounts of coke deposits accumulated on the catalysts after 6 h TOS are listed in Table 2. Clearly, more coke was detected on the catalysts used in the absence of O_2. The carbonaceous deposits accumulated on Pt/ZrO_2 (0.9 wt%) were greater than those deposited on Pt/CeO_2 (0.7 wt%) despite the same TOS. Addition of 1% O_2 resulted in a similar trend, i.e., less coke was found when CeO_2 was used as a support.

In order to investigate the coke on the spent catalysts, MALDI-TOF MS spectra of the carbonaceous deposits were recorded. Fig. 9a compares the spectra corresponding to coke deposits on Pt/ZrO_2 in the presence and absence of O_2 during steam reforming. Both spectra reveal a broad molecular weight distribution up to 600 m/z, which was the largest mass recorded. In the presence of oxygen, the dominating mass signals were found below 300 m/z. In contrast, the spectrum corresponding to the coke formed during steam reforming in the absence of oxygen shows that the strongest peaks appear above 400 m/z. Similar trends were observed for the Pt/CeO_2 catalyst (Fig. 9b). A main peak around 300 m/z was observed in the spectrum associated to the coke developed in oxidative conditions, whereas the dominating species in the absence of oxygen was observed around 450 m/z.

Table 2
Coke amount after 6 h time on stream over Pt/ZrO_2 and Pt/CeO_2.

Catalyst	Percentage of coke deposited (%)	
	Presence of O_2	Absence of O_2
Pt/ZrO_2	0.6	0.9
Pt/CeO_2	0.3	0.7

GHSV = 80 000 h^{-1}; T = 700 °C; S/C = 5.

4. Discussion

One of the main issues in the production of H_2 *via* steam reforming of bio-oil-based compounds is the development of a stable catalyst [8,19]. In this work, the stability of Pt-based catalysts for steam reforming of AcOH, a model component in bio-oil, has been studied in detail. A close look at the catalytic results

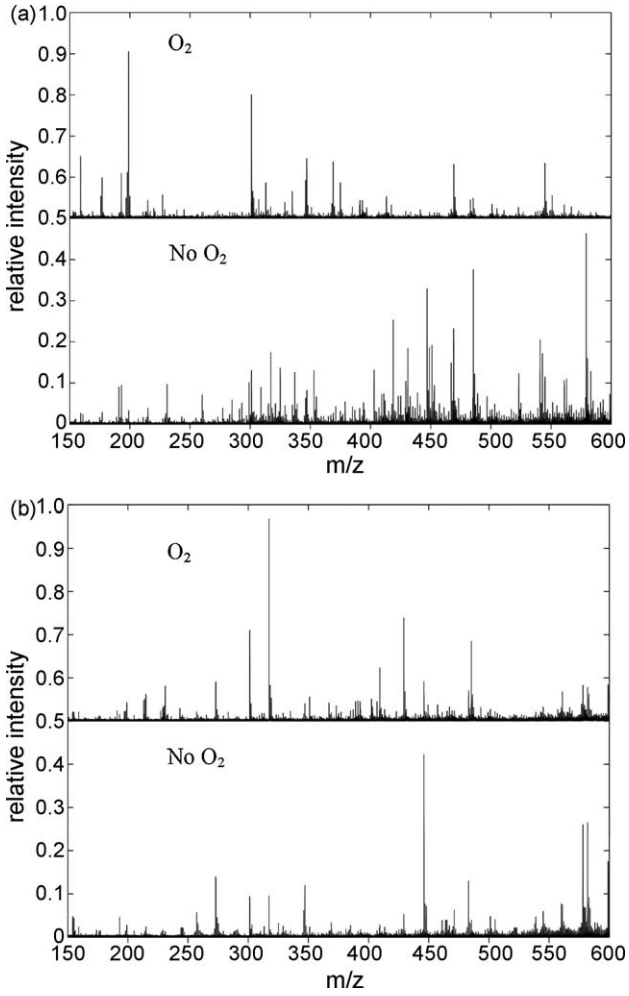

Fig. 9. MALDI-TOF MS spectra of coke deposited on (a) Pt/ZrO_2 and (b) Pt/CeO_2 during the steam reforming of AcOH in the presence and absence of oxygen.

(Figs. 5–7) shows that Pt-based catalysts presented very high activity, with complete conversion of AcOH at high space velocity and initial TOS. We have shown earlier that a bi-functional mechanism is operative for Pt-based catalysts in steam reforming of acetic acid [6,7,20]. Acetic acid decomposes over Pt to result in sorbed CH_x specie [20], which are reformed by hydroxyl groups generated on the support oxide in the presence of water. Reasonable amounts of H_2 were observed over ZrO_2 (Fig. 4a) and CeO_2 (Fig. 6a) suggesting that these supports have some steam reforming activity. Comparable observations were reported by Basagiannis and Verykios [21] for the steam reforming of AcOH over Al_2O_3 type materials at similar reaction conditions.

Unfortunately, the support oxide (ZrO_2 or CeO_2) also catalyses two undesirable reactions of AcOH: (i) decomposition to CO_2 and CH_4 and (ii) condensation, namely ketonization, to produce acetone. Both routes have been reported earlier over metal oxide materials [22–24] in line with our results (Figs. 4a and 6a).

The presence of Pt clearly enhanced steam reforming and WGS reactions, as evidenced by an initial product composition near thermodynamic equilibrium (Figs. 5a and 7a). The low amounts of CH_4 observed over Pt/ZrO_2 and Pt/CeO_2 as compared to those over the corresponding supports could be explained by the fact that Pt-based catalysts are excellent for the steam reforming of methane [25]. Rioche et al. [26] carried out steam reforming of AcOH over 1 wt% $Pt/CeZrO_2$ around 700 °C with S/C ratio of 2. They observed a H_2/CO ratio lower than in our case. CO concentration normally decreases when increasing the S/C ratio at a given temperature. The lower S/C ratios in their study can explain the differences observed.

The use of ZrO_2 as a support (Fig. 4a) did not result in stable catalyst activity under our conditions. Acetone appeared as a product during deactivation and disappeared again when the reactor system reached levels of gas phase homogeneous reactions. It is known that ZrO_2 is active in the ketonization of AcOH to lead to acetone [23,24]. Acetone exhibits high chemical reactivity on metal oxides, and further condensation reactions (C–C bond coupling) cannot be suppressed. This yields to oligomeric non-volatile specie that then result in deactivation of the catalyst [22,27,28]. Scheme 1 shows reaction routes during steam reforming of acetic acid and formation/consumption of acetone.

Over a fresh catalyst, steam reforming of acetone (k_5) is significant, as seen from experiments using acetone as feed (Fig. 8a). Parallel, acetone formed is also converted to oligomeric coke specie (k_4). Thus, the absence of acetone in the beginning of the reaction suggests that the routes for the disappearance of acetone, i.e., condensation reactions and/or steam reforming (routes 4 and 5, respectively) are faster than its formation (route 2). We reported earlier [7] that the active sites for the steam reforming of AcOH over Pt/ZrO_2 are the boundaries between the metal and the support. As soon as the coke blocks those areas, the routes associated with steam reforming (k_1 and k_5) are suppressed. Acetone is then observed in the gas phase (k_3). Part of the support is still available to convert AcOH to acetone (route 2) and further to coke. At a certain instant, however, this will block all support sites in such way that AcOH will not be further converted catalytically and no acetone will be formed. Only gas phase (non-catalytic) reactions will occur at this stage. After catalyst deactivation we indeed observed only gas phase contribution into acetic acid conversion (Figs. 5a and 7a).

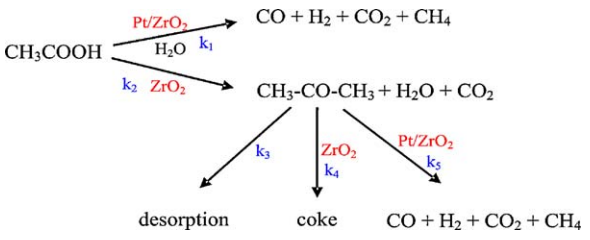

Scheme 1. Reaction scheme of the catalytic steam reforming of acetic acid over Pt/ZrO_2. For details of coking (k_4) see Scheme 2.

Under comparable conditions (750 °C, S/C ratio 3), Vagia and Lemonidou [29] reported 23% thermal cracking conversion of AcOH, in line with our findings (Fig. 3a). However, they observed higher amounts of H_2 and CH_4 and they did not report formation of undetectable gases. At high temperatures and in the absence of catalyst, formation of tars is very likely. These compounds are volatile at these high temperatures; however, they condense below 350–400 °C. Indeed exit of the reactor showed accumulation of some black deposits, indicating that oligomer/condensate formation occurred in our case. This led to poor "C" balance (~85%). Other authors [30,31] have shown very high or even complete conversion of AcOH at 700 °C in the absence of catalyst. These results indicate that thermal decomposition depends on a variety of factors such as temperature, steam to carbon ratio, contact time, void volume, etc. An exact comparison is not straightforward.

The stability of CeO_2-based catalyst is certainly improved as compared to Pt/ZrO_2 (Figs. 5a and 7a). Interestingly, acetone was also observed in the case of Pt/CeO_2, but only in traces (Fig. 7a). According to Scheme 1, this would imply that (i) Pt/CeO_2 is able to steam reform acetone much better than Pt/ZrO_2 (k_5) and (ii) the route for acetone condensation to lead to coke deposits is less significant (k_4). Our results on the steam reforming of acetone (Fig. 8a and b) support the first argument. In this way, Pt/CeO_2 is indirectly minimizing the formation of carbonaceous deposits. At the same time we cannot rule out the possibility that less acetone is formed over CeO_2 (k_2).

The combination of the red-ox properties of CeO_2 (Fig. 1) along with the potential of H_2O to re-oxidize CeO_2, as demonstrated by TPR/TPO experiments in Fig. 2, is a possible reason that coke deposition is less significant. It is of general knowledge that CeO_2 has excellent oxygen exchange capacity involving red-ox changes between Ce^{4+} and Ce^{3+} [32]. We thus, propose that CeO_2 is able to supply oxygen in order to combust coke deposits resulting in oxygen vacancies. Dissociation of H_2O leads to the regeneration of the oxygen vacancies. Thus, accumulation of coke deposits on the catalyst surface is minimized.

Oxygen addition to steam reform feed improved the stability of nearly all systems, as evidenced by the changes in TOS (Figs. 4–7). Others have reported such improvements in catalyst stability. Cavallaro et al. [9] also observed a positive effect of oxygen addition on the stability of nobel-metal-based catalysts (Rh/Al_2O_3) in the steam reforming of ethanol at 650 °C. The decrease in H_2 yield due to the presence of oxygen is in agreement with literature. Vagia and Lemonidou [33] reported a decrease in H_2 yield around 19% based on thermodynamic calculations on the autothermal steam reforming of AcOH at the same conditions used in this investigation, i.e., 700 °C and a O_2/AcOH ratio of 0.4.

Even though the presence of oxygen improved the catalyst lifetimes, Pt/ZrO_2 still suffered from rapid deactivation after 3 h TOS (Fig. 5b). The profile was similar to that observed in the absence of oxygen (Fig. 5a). Acetone was observed in a comparable trend, suggesting that the mechanism of deactivation is the same. In the presence of oxygen, no acetone was observed in the case of Pt/CeO_2 (Fig. 7b); as expected, it showed excellent stability for the steam reforming of acetic acid. Furthermore, in the presence of oxygen, the decrease in hydrogen yield was limited (H_2 yield decreased from 85% to 75%) and coke was combusted to a larger extent. Pt/CeO_2 is thus a promising catalyst for the steam reforming of biomass-based oxygenates.

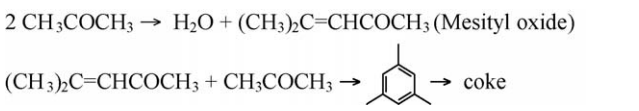

Scheme 2. Reactions scheme of formation of polyaromatics over metal oxide (k_4 from Scheme 1).

Enhanced stability of the spent catalysts is directly related to the lower extend of coking in the presence of oxygen (Table 2). Accordingly, the least amount of coke was observed on Pt/CeO_2, which was also the most stable. Evidences for a decrease in coke deposition in the steam reforming of oxygenates (ethanol) in the presence of oxygen have been reported in previous papers [9,34]. They proposed a mechanism of auto-cleaning (*in situ* coke combustion) of the catalytic surface by the oxygen, which is also relevant in our case.

It is relevant at this point to understand if there are differences in the chemical characteristics of coke for the different catalyst systems studied and if correlations can be drawn as to their stability. As mentioned earlier, during steam reforming, coke mostly results from a cascade of condensation and oligomerization reactions over the support [6,21,22,27,35]. Scheme 2 summarizes these reactions.

MALDI-TOF MS spectra of coke from both Pt/ZrO_2 (Fig. 9a) and Pt/CeO_2 (Fig. 9b) catalysts clearly show that under oxidative conditions, oligomerization/ageing occur to a lower extent since the spectra are dominated by lower molecular weight specie. This might be due to the fact that continuous *in situ* combustion of coke/coke precursors keeps their levels lower. Lower molecular weight coke specie are expected to be more reactive and can be gasified more easily by oxygen.

To summarize, Pt/ZrO_2 catalyst improved stability with the presence of oxygen (compare Fig. 5a and b). However, deactivation also occurred after longer TOS (Fig. 5b). On the other hand, Pt/CeO_2, catalyst with red-ox capability, showed excellent stability under oxidative conditions (Fig. 7b). Furthermore, Pt/CeO_2 enhanced steam reforming of coke precursors, acetone in our case (Fig. 8b). Therefore, we propose that the combination of (i) enhanced steam reforming activity of acetone (coke precursor), (ii) oxygen addition to the steam reforming feed and the (iii) red-ox characteristics of CeO_2 to use both oxygen and water as oxidants, are the key reasons to justify the excellent catalytic stability of Pt/CeO_2. This catalyst shows promise for the steam gasification of more complex biomass-derived oxygenates that are currently under study.

5. Conclusion

Our findings demonstrate that the nature of the support has a strong influence on the catalyst stability in the steam reforming of AcOH. Using a catalyst support with red-ox properties improves catalyst lifetime. Enhanced steam reforming of acetone, a coke precursor, and minimization of carbonaceous specie formed are reasons for extended catalyst life. Catalyst stability can be further improved by the addition of oxygen in the feed to allow *in situ* combustion of coke formed. Presence of oxygen also minimizes the extent of oligomerization/ageing leading to coke specie more reactive to gasification. The enhanced steam reforming activity and red-ox characteristics that allow the use of water as an oxidant for coke combustion/gasification make Pt/CeO_2 a promising catalyst for the steam reforming of biomass-based oxygenates.

Acknowledgements

This work was financially supported by the Netherlands Organisation of Scientific Research (NWO) through the ACTS (Advanced Chemical Technologies for Sustainability) program. The authors thank Ing. L. Vrielink for BET, XRF measurements and Ing. B. Geerdink for technical support.

References

[1] M. Balat, Energy Sources A: Recovery, Utilization, and Environmental Effects 30 (2008) 552–564.
[2] G.Q. Lu, J.C. Diniz da Costa, M. Duke, S. Giessler, R. Socolow, R.H. Williams, T. Kreutz, Journal of Colloid and Interface Science 314 (2007) 589–603.
[3] C.A. Mullen, A.A. Boateng, Chemical composition of bio-oils produced by fast pyrolysis of two energy crops, Energy and Fuels (2008) 2104–2109.
[4] F J.P. Diebold, A review of the toxicity of biomass pyrolysis liquids formed at low temperatures, Fast Pyrolysis of Biomass: A Handbook, Newbury, UK, 2003, pp. 135–163.
[5] F.A. T. Milne, M. Davis, S. Deutch, D. Johnson, Developments in Thermochemical Biomass Conversion, London, 1997, pp. 409–424.
[6] K. Takanabe, K. Aika, K. Seshan, L. Lefferts, Journal of Catalysis 227 (2004) 101–108.
[7] K. Takanabe, K.-I. Aika, K. Inazu, T. Baba, K. Seshan, L. Lefferts, Journal of Catalysis 243 (2006) 263–269.
[8] K. Takanabe, K.-I. Aika, K. Seshan, L. Lefferts, Chemical Engineering Journal 120 (2006) 133–137.
[9] S. Cavallaro, V. Chiodo, S. Freni, N. Mondello, F. Frusteri, Performance of Rh/Al_2O_3 catalyst in the steam reforming of ethanol: H_2 production for MCFC, Applied Catalysis A: General (2003) 119–128.
[10] S.M. de Lima, I.O. da Cruz, G. Jacobs, B.H. Davis, L.V. Mattos, F.B. Noronha, Journal of Catalysis 257 (2008) 356–368.
[11] D. Haffad, A. Chambellan, J.C. Lavalley, Journal of Molecular Catalysis A: Chemical 168 (2001) 153–164.
[12] F. Sadi, D. Duprez, F. Gérard, A. Miloudi, Journal of Catalysis 213 (2003) 226–234.
[13] G. Vlaic, R. Di Monte, P. Fornasiero, E. Fonda, J. Kaspar, M. Graziani, Journal of Catalysis 182 (1999) 378–389.
[14] M.H. Yao, R.J. Baird, F.W. Kunz, T.E. Hoost, Journal of Catalysis 166 (1997) 67–74.
[15] C. Sievers, I. Zuazo, A. Guzman, R. Olindo, H. Syska, J.A. Lercher, Journal of Catalysis 246 (2007) 315–324.
[16] M. Boaro, M. Vicario, C. de Leitenburg, G. Dolcetti, A. Trovarelli, Catalysis Today 77 (2003) 407–417.
[17] T. Caputo, L. Lisi, R. Pirone, G. Russo, Applied Catalysis A: General 348 (2008) 42–53.
[18] C.D. Leitenburg, A. Trovarelli, J. Kaspar, Journal of Catalysis 166 (1997) 98–107.
[19] B. Matas Güell, I.M. Torres da Silva, K. Seshan, L. Lefferts, Applied Catalysis B: Environmental (2008), doi:10.1016/j.apcatb.2008.09.018.
[20] B. Matas Güell, I. Babich, K. Seshan, L. Lefferts, Journal of Catalysis 257 (2008) 229–231.
[21] A.C. Basagiannis, X.E. Verykios, Applied Catalysis B: Environmental 82 (2008) 77–88.
[22] S. Lippert, W. Baumann, K. Thomke, Journal of Molecular Catalysis 69 (1991) 199–214.
[23] M. Gliński, J. Kijeński, Reaction Kinetics and Catalysis Letters 69 (2000) 123–128.
[24] K. Parida, H.K. Mishra, Journal of Molecular Catalysis A: Chemical 139 (1999) 73–80.
[25] J.R. Rostrup-Nielsen, Catalysis: Science and Technology 5 (1984) 1–117.
[26] C. Rioche, S. Kulkarni, F.C. Meunier, J.P. Breen, R. Burch, Applied Catalysis B: Environmental 61 (2005) 130–139.
[27] M.A. Aramendía, V. Borau, C. Jiménez, A. Marinas, J.M. Marinas, J.R. Ruiz, F.J. Urbano, Journal of Molecular Catalysis A: Chemical 218 (2004) 81–90.
[28] L.M. Gandía, M.A. Vicente, A. Gil, Applied Catalysis B: Environmental 38 (2002) 295–307.
[29] E.C. Vagia, A.A. Lemonidou, Applied Catalysis A 351 (2008) 111–121.
[30] J.R. Galdamez, L. Garcia, R. Bilbao, Energy and Fuels 19 (2005) 1133–1142.
[31] D. Wang, D. Montane, E. Chornet, Applied Catalysis A: General 143 (1996) 245–270.
[32] K. Nagaoka, K. Seshan, K. Takanabe, K.-I. Aika, Catalysis Letters 99 (2005) 97–100.
[33] E.C. Vagia, A.A. Lemonidou, International Journal of Hydrogen Energy 33 (2008) 2489–2500.
[34] S. Cavallaro, V. Chiodo, A. Vita, S. Freni, Journal of Power Sources 123 (2003) 10–16.
[35] K.M. Dooley, A.K. Bhat, C.P. Plaisance, A.D. Roy, Applied Catalysis A: General 320 (2007) 122–133.